

Shape My Moves: Text-Driven Shape-Aware Synthesis of Human Motions

Ting-Hsuan Liao^{1, 2*} Yi Zhou² Yu Shen² Chun-Hao Paul Huang² Saayan Mitra²
 Jia-Bin Huang¹ Uttaran Bhattacharya²
¹ University of Maryland, College Park, USA ² Adobe Research

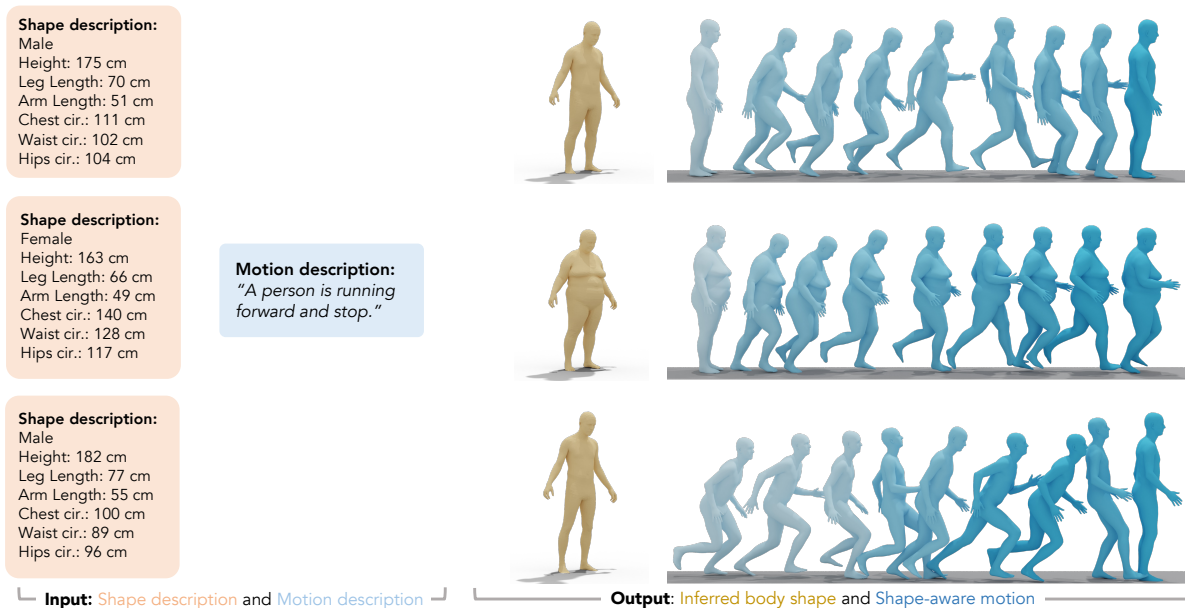


Figure 1. Text-Driven Shape-Aware Motion Synthesis. The same motion performed by different body shapes can vary significantly, a realism aspect often overlooked in text-to-motion tasks. We propose a novel framework to integrate both shape and motion descriptions as input. Our framework synthesizes the shape parameters to reflect the described physical attributes, and injects them into motion synthesis to generate plausible shape-aware motions. The figure demonstrates the same *running* motion synthesized across different body shapes.

Abstract

We explore how body shapes influence human motion synthesis, an aspect often overlooked in existing text-to-motion generation methods due to the ease of learning a homogenized, canonical body shape. However, this homogenization can distort the natural correlations between different body shapes and their motion dynamics. Our method addresses this gap by generating body-shape-aware human motions from natural language prompts. We utilize a finite scalar quantization-based variational autoencoder (FSQ-VAE) to quantize motion into discrete tokens and then leverage continuous body shape information to de-quantize these tokens back into continuous, detailed motion. Additionally, we harness the capabilities of a pretrained language model to predict both continuous shape parameters and motion to-

kens, facilitating the synthesis of text-aligned motions and decoding them into shape-aware motions. We evaluate our method quantitatively and qualitatively, and also conduct a comprehensive perceptual study to demonstrate its efficacy in generating shape-aware motions. Project URL: <https://shape-move.github.io/>.

1. Introduction

Human motion synthesis is an expansive field with wide applications in avatar creation, robotics, and the gaming industry [27, 63, 75, 83]. Advances in both motion synthesis methods and language modeling techniques have, in recent times, led to the development of text-to-motion synthesis, with the aim of generating dynamic motions that are con-

textually aligned with textual descriptions.

Previous efforts in text-to-motion synthesis have explored techniques to integrate motion and language. Some approaches map motion and language into a shared latent space, and then sample motions from it based on text inputs [5]. Others utilize diffusion models conditioned on learned features, such as CLIP, to enhance the quality and relevance of the generated motions [85]. To overcome the difficulties of learning continuous motion features, quantizing motions into discrete tokens has emerged as an area of significant interest, which can then be predicted using transformers [105] or fine-tuning large language models [50]. These advancements have led to improved realism and creative control over motion synthesis.

However, existing methods typically standardize motions by mapping to a canonical human body model. This results in homogenized motions across diverse body types and leaves out the unique attributes of individual body shapes. In reality, persons with different body shapes perform the same action with distinct physiological differences, as illustrated in Figure 1. Treating these distinct motions identically during motion synthesis leads to artifacts in subsequent motion transfer efforts [6], often resulting in unrealistic motions and limitations on the body shapes on which the motions can be reliably retargeted.

Incorporating body shapes in motion synthesis is challenging due to the difficulties in both obtaining closed-form parameterization of motions by body shapes and learning the coarse-to-fine differences in motions due to individual body shapes in a data-driven manner. The challenges are exacerbated when attempting to merge continuous shape representations with quantized motion representations. To address these hurdles, we propose a quantization-based framework that seamlessly integrates continuous body shape data and thereby manages the information loss due to motion quantization. Consequently, our model not only predicts discrete motion tokens but also accurately captures continuous human body shape data, significantly enhancing the realism and individualism of synthesized motions.

Our model also leverages the capabilities of large language models to process complex language and predict sequential data, while handling continuous information through its latent space. This dual ability allows our model to predict continuous body shape parameters alongside discrete motion tokens. To maximize the benefits of this dual capability, our task-specific decoder utilizes discrete tokens and continuous shape parameter predictions as conditions to generate shape-aware human motions.

To summarize, our main contributions include:

- End-to-end synthesis of both body shape parameters and shape-aware motions from input text descriptions.
- A novel framework to combine continuous shape and quantized motion data for efficient learning.

- Demonstrating efficacy through thorough quantitative and qualitative evaluations and human perceptual studies.

2. Related Work

We summarize existing research in the related areas of motion transfer, motion generation with and without body shape information, and motion generation from text inputs.

Motion Transfer. Motion transfer is a common strategy for applying motions from a source skeletal topology to a target one. While heuristic approaches based on inverse kinematics can resolve minor motion artifacts in the target skeleton, they cannot reliably reconcile motion artifacts due to topological mismatches between the source and the target [24, 27, 63, 75]. More direct approaches that require paired source and target motion data are limited by the practical challenges of obtaining such paired data, particularly as the topological differences between the source and the target skeletons increase [1, 97, 108]. Recent data-driven approaches relying on deep learning techniques [6] can alleviate the strict requirements of paired motion data [3, 54], and can even transfer motions between different modalities, such as from videos to 3D meshes [2, 22], while plausibly adhering to physical constraints, such as foot contacts [14, 94]. However, such approaches predominantly rely on skeletal topologies to transfer motions. They either cannot adapt to motion transfer between physiologically different body shapes or can only do so for a limited variety of body shapes and motions [38, 72, 95, 104].

Human Motion Generation with Body Shapes. We broadly categorize computational methods for human motion generation into *shape-aware* — those that consider body shapes in the generation process, and *shape-free* — those that generate motions for a normalized representation of the human body and use motion transfer techniques to apply the generated motions to different body shapes. Owing to the simpler nature of its formulation, shape-free motion generation has been richly explored in computer vision and graphics. The underlying motion models are often developed with physically-based constraints [15, 30, 80, 81, 87, 98–101, 103] and employ reinforcement learning frameworks for use within physics engines [61, 65–67, 77, 78, 96]. In addition to physical constraints, generative approaches are typically conditioned on guidance signals, such as past motions of the same person [52] interactive motions of another person [35, 84], audio, including music [16, 55] and speech [18, 37], text descriptions [5, 32, 33], and their various combinations [17]. The scope of these approaches has expanded from deterministic, producing a fixed output for a given set of guidance signals [8, 12, 29, 36, 39, 41, 42, 48], to stochastic, enabling

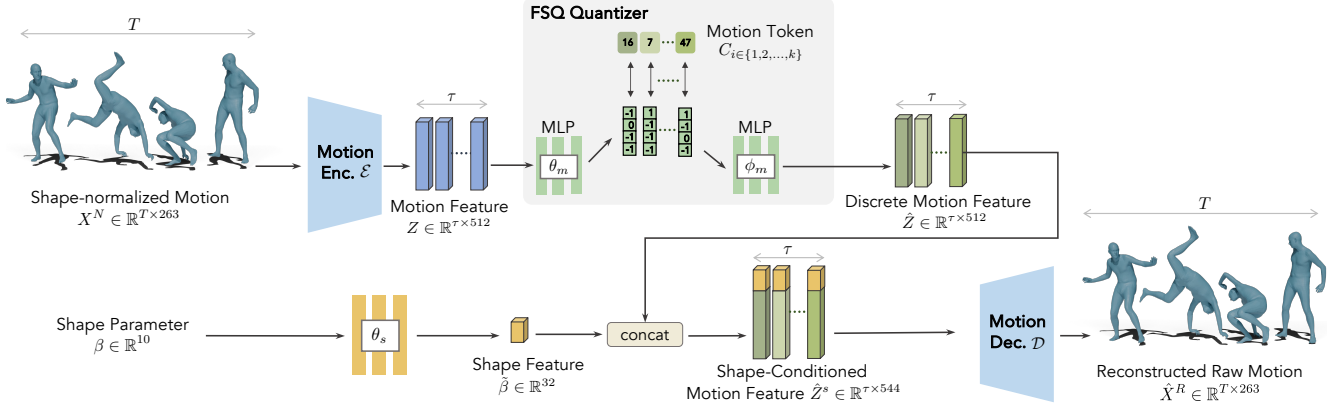


Figure 2. **Shape-Aware FSQ-VAE (SA-VAE) Overview.** SA-VAE is our quantization network learning to generate discrete motion tokens. Given a shape-normalized motion $X^N \in \mathbb{R}^{T \times 263}$ of length T and dimensionality D ($= 263$ in our setup), we first encode the motion with the Motion Encoder \mathcal{E} into a motion feature $Z \in \mathbb{R}^{\tau \times D}$, where τ represents a downsampling of T . We leverage the FSQ [62] quantizer to quantize Z , which gives a discrete feature \hat{Z} . The MLP_{θ_m} and MLP_{ϕ_m} transform the features into the required code dimensions. To condition on the shape, we project the shape parameter β with the Projector P_{θ_s} to align with \hat{Z} . We concatenate the shape feature $\hat{\beta}$ with \hat{Z} , then feed it into the Motion Decoder \mathcal{D} to predict the reconstructed motion \hat{X}^R .

more creative control over the generated motions [9, 43, 46, 74]. Generative frameworks such as GANs and VAEs, paired with the creation of standardized human representations [56] and large-scale benchmark datasets [60], have heralded the modern wave of motion generation methods. They have significantly improved the plausibility of generated motions on canonical skeletons [4, 13, 73], and have been expanded to object [34] and scene interactions [51]. More recent methods have leveraged versatile sequence modeling architectures such as transformers [58] and robust generative techniques such as denoising diffusion models [26]. Despite the remarkable progress in shape-free motion generation, their effective realism, when applied to diverse body shapes, remains susceptible to common motion artifacts, including self-intersections, foot contact errors, and unnatural pose articulations. Shape-aware pose models [25, 40, 109] and motion generation methods [88] have made progress in reducing this quality gap by explicitly incorporating body shape information in the generative process and employing physically-based constraints that support the shape information. Our work takes the next step in shape-aware motion generation by learning to generate motions from natural language descriptions of both shapes and motions in an end-to-end fashion.

Motion from Language Models. Motion generation from text descriptions has become especially active in recent human motion generation research, aided largely by the user-friendliness and creative utility of describing motions in free-form text via language models [5, 10, 11, 44, 68, 69, 85, 107]. Current state-of-the-art approaches typically employ diffusion-based [23, 76, 79, 86, 106] networks

or transformer-based [45, 50, 105] networks that map tokenized language features to motion features. In the quantization step, motion features are also often quantized and tokenized, following quantization paradigms such as the VQ-VAE [93], to expedite the generative learning process while maintaining motion quality. We inject shape-awareness into the motion tokenization process through data-driven shape features and finite scalar quantization (FSQ) [62], enabling us to map language tokens to combine shape and motion features for shape-aware motion generation from text.

3. Method

We aim to generate both human body shapes and motions from natural language text descriptions. To this end, we first preprocess text-to-motion data to obtain shape descriptions and shape-aware motion data (Section 3.1). We propose a two-stage framework for shape-aware motion synthesis from text, consisting of a shape-aware FSQ-VAE (SA-VAE) and a shape-motion token predictor (ShapeMove). The SA-VAE efficiently quantizes shape-normalized motion into discrete tokens and reconstructs motions from shape parameters (Section 3.2). ShapeMove generates both shape tokens and a sequence of motion tokens that accurately correspond to the text description (Section 3.3).

3.1. Data Preprocessing

Existing text-motion datasets only provide natural language labels to describe motions [43, 70]. To obtain specific text labels for body shape, we utilize the SMPL [56] model’s shape parameters β , which control the body shape, and extract the measurements of six attributes to get a holistic view of the body: height, arm and leg lengths, and chest, waist,

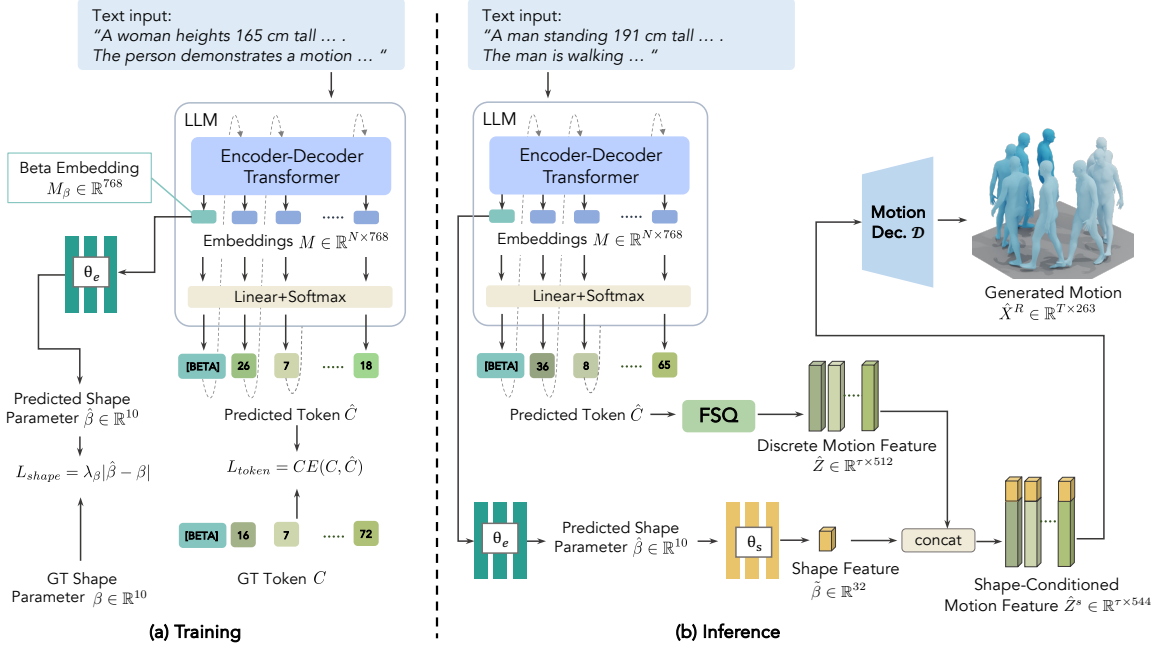


Figure 3. **ShapeMove Overview.** In the training phase (a), the transformer network takes in the text inputs describing human motions and body shapes and predicts quantized motion tokens and the shape token [BETA]. The embedding for [BETA] passes through the Projector P_{θ_e} to predict the shape parameter $\hat{\beta}$. We use cross-entropy loss for comparing ground truth tokens C with predicted tokens \hat{C} , and $L1$ loss for shape parameter to optimize the model. In the inference phase (b), our model predicts motion tokens \hat{C} and the shape parameter $\hat{\beta}$ from text inputs. We de-quantize these tokens using FSQ, and project into shape parameters with Projector P_{θ_s} . We concatenate $\hat{\beta}$ and \hat{C} , and decode into the generated motion sequence with the Motion Decoder \mathcal{D} . Our model effectively synthesizes shape parameters and shape-aware motions reflecting the physical form and actions described in the input text.

and hip circumferences. These attributes form our shape description, which we use as input for the model.

Since available text-motion datasets contain a limited diversity of characters, we propose generating additional body shapes for training. We utilize the Attributes to Shape (A2S) model of Shap [25], which can generate SMPL beta values from linguistic shape attributes to generate more body shapes in a controlled and plausible manner. We detail the pipeline for using additional shapes in Section 3.2.

For the motion representation, we follow the preprocessing procedure of Guo *et al.* [43], extracting joint positions from the SMPL layer and computing motion representations with shape $T \times D$, where $D=263$ is the data dimension and T is the number of motion frames. Each motion representation contains root relative rotation and velocity, root height, joint locations, velocities, rotations, and foot contact labels. Notably, we skip the normalizing step of canonicalizing the skeletons to a homogeneous body shape. We denote this as the shape-aware motion X^R , and the corresponding shape-normalized version of the motion as X^N .

3.2. Shape-Aware FSQ-VAE (SA-VAE)

Quantizing motion into discrete tokens has led to significant progress in the text-to-motion synthesis [44, 50, 105].

Existing approaches quantize motion into discrete tokens and then predict sequences of motion tokens that align with the text input. However, the codebook capacities of these approaches are insufficient for reconstructing shape-variant motions (X^R). To address this limitation, we propose a new framework, Shape-Aware FSQ-VAE (SA-VAE), to effectively quantize the shape-normalized motions X^N into discrete tokens and reconstruct shape-aware motions \hat{X}^R by conditioning on shape information. We use X^N instead of X^R as the SA-VAE input as it enables the SA-VAE to disentangle the *content* (given by the pose sequences) and the *style* (given by the body shapes) components of the motions, focusing on learning tokens for the motion content and shape features for the motion style separately, and then combining them for efficient decoding into X^R .

As illustrated in Figure 2, our SA-VAE comprises a motion encoder \mathcal{E} and a motion decoder \mathcal{D} . To learn a more generalized motion codebook, the encoder \mathcal{E} takes in a sequence of shape-normalized motion frames $X^N = [x_1^N, x_2^N, \dots, x_T^N]$, $x_i^N \in \mathbb{R}^D$ and encodes them into motion features $Z = [z_1, z_2, \dots, z_\tau]$, $z_i \in \mathbb{R}^d$ and τ representing a downsampling of T .

We utilize Finite Scalar Quantization (FSQ) [62] as our quantizer, given its superior codebook utilization without

needing the additional regularization typically used in previous quantizers [105]. We denote the quantized features as $\hat{Z} = \text{MLP}_{\phi_m}(\nabla[f(\text{MLP}_{\theta_m}(Z))]_{ste})$, where f is a bounding function that confines the latent within a specific range, defined as $f[L/2] \odot \tanh(Z)$, and $L \in \mathbb{Z}^\ell$ determines the width of the codebook for each dimension. We round the latents to integers with straight-through gradients $(\nabla[\cdot]_{ste})$. The MLPs, MLP_{θ_m} and MLP_{ϕ_m} , transform the features into required code dimensions.

Our motion decoder \mathcal{D} decodes the discrete motion features $\hat{Z} = [\hat{z}_1, \hat{z}_2, \dots, \hat{z}_\tau]$, $\hat{z}_i \in \mathbb{R}^d$ into shape-aware motions. To incorporate shape information, we extract the shape feature $\tilde{\beta} = \text{P}_{\theta_s}(\beta)$, where P_{θ_s} is an MLP-based projector. We concatenate the shape feature along the time dimension with the discrete motion feature to feed into \mathcal{D} . We denote the final reconstructed shape-aware motion as $\hat{X} = \mathcal{D}(\hat{Z} \oplus \tilde{\beta})$, \oplus denoting concatenation.

Objective. Following the approach of T2M-GPT [105], we use L_1^{smooth} to compute the reconstruction loss L_r between the ground truth and the reconstructed motions to train the SA-VAE. Denoting X_{rot} as the invariant rotation information of X , we write the reconstruction loss as

$$L_r = L_1^{\text{smooth}}(X, \hat{X}) + \lambda_{\text{rot}} L_1^{\text{smooth}}(X_{\text{rot}}, \hat{X}_{\text{rot}}), \quad (1)$$

where λ_{rot} is a hyperparameter to balance the two losses. We also design physical losses to constrain the physical aspects of the reconstructed motion. Similar to [88, 90, 102], we include the floating loss L_{float} , the foot sliding loss L_{slide} , and the bone length loss L_{bone} as geometric losses. L_{float} minimizes the per-frame distance of the lowest joints above the ground from the ground plane. L_{slide} minimizes the ground velocity of the foot joint if they are determined to be in ground contact using a distance threshold from the ground. L_{bone} minimizes the deviation of bone lengths between the ground truth and the reconstructed motions. We write the final objective as

$$L_{\text{vq}} = L_r + \lambda_f L_{\text{float}} + \lambda_s L_{\text{slide}} + \lambda_b L_{\text{bone}}, \quad (2)$$

where λ_f , λ_s , and λ_b are the loss-balancing hyperparams.

Shape Data Augmentation. To provide our SA-VAE with a wide diversity of subjects with different body shapes, beyond what is available in datasets, we adopt a data augmentation strategy. We replace $q\%$ of the ground-truth shape parameters with synthetically generated ones, as mentioned in Section 3.1. Since there is no corresponding ground truth motion for the augmented shapes, we only optimize the indices with L_{slide} and L_{bone} .

3.3. Shape-Aware Motion Synthesis (ShapeMove)

With the SA-VAE, we can tokenize a sequence of motion $[x_1^N, x_2^N, \dots, x_T^N]$ into a sequence of discrete indices $[c_1, c_2, \dots, c_\tau]$. Subsequently, our framework, ShapeMove, learns to map from language to shape-aware motion representations. We adopt a pretrained language model to predict the sequence of tokens. We illustrate the overview of ShapeMove in Figure 3. To fine-tune the language model to understand the relationships between motion, shape, and text, we expand the original language model’s vocabulary by adding $k + 2$ motion vocabulary items. Here, k is the number of codes from the quantizer codebook, and the additional two tokens are special tokens to signify the start and end of the motion token sequence. We also add one shape vocabulary token, [BETA], to represent the shape. The language model takes text tokens as input and predicts tokens $\{\text{[BETA]}, \hat{C}\}$. We design the ground truth tokens to be $\{\text{[BETA]}, C\}$, *i.e.*, we append the [BETA] token with a sequence of motion tokens that align with the text input. We fine-tune the language model in an autoregressive manner.

Since shape parameters are fixed for a given body shape, unlike motion prediction, we cannot formulate shape parameter prediction as predicting a sequence of tokens. Representing shape would require an impractically large codebook, akin to using discrete numbers to fit a continuous space. To address this, previous works show that the last embedding in the language model can contain continuous information [28, 53]. Instead of attempting to learn a discrete representation for shape, we extract the information through embedding. We denote the predicted output token as \hat{C}_i , the corresponding embedding as M_i , and the embedding corresponding to [BETA] as M_β . We obtain the shape parameter through a projector P_{θ_e} , yielding $\hat{\beta} = \text{P}_{\theta_e}(M_\beta)$.

Objective. To enable the language model to learn semantically consistent shape and motion vocabularies, we design the training data as mentioned in Section 3.1. The target outputs are the corresponding ground truth shape parameters and motion tokens. We train the model with the following objectives:

$$L_{\text{token}} = \text{CrossEntropy}(C, \hat{C}) \quad (3)$$

$$L_{\text{shape}} = \lambda_\beta |\beta - \hat{\beta}|, \quad (4)$$

where L_{token} is the cross-entropy loss maximizing the log-likelihood of predicting the motion tokens, L_{shape} is the L_1 norm difference between the ground truth and the estimated shape parameters, and λ_β is the hyperparameter balancing the shape loss.

Table 1. **Comparison with Baselines.** We evaluate the Penetrate, Float, Skate Ratio, and Bone Length Variances for our method and available baselines. For fair comparison, retrain baselines with shape-aware motions. The *Shape Input Capability* column indicates methods that can incorporate both shape and motion descriptions — a \times here suggests the corresponding text encoder cannot parse shape descriptions. *Arbitrary Length* denotes results obtained without using ground-truth motion lengths. We compare with methods that share the same constraints as ours, capable of generating arbitrary motion lengths and accepting shape descriptions as input. Our method achieves the best or comparable results across the board. It particularly excels in the Penetrate metric, showcasing its adeptness at handling shape-aware motions. █ and █ highlight the best and second-best results.

Methods	Shape Input Capability	Arbitrary Length	Penetrate (cm) \downarrow	Float (cm) \downarrow	Skate (%) \downarrow	Bone Length Variances \downarrow	RPrecision \uparrow			FID \downarrow	MMDist \downarrow	Diversity \downarrow
							Top1	Top2	Top3			
Real	—	—	0.0	0.0362	7.468	0.0	0.469	0.665	0.769	0.001	3.217	0.000
SA-VAE (Recon.)	—	—	0.0289	0.2090	6.443	0.623	0.454	0.645	0.749	0.125	3.308	0.101
TM2T [44]	\times	✓	0.1485	0.2456	8.554	5.339	0.374	0.559	0.673	1.671	3.843	0.937
T2M [43]	\times	✓	0.0939	0.6805	4.250	1.352	0.408	0.592	0.697	1.230	3.597	0.430
MLD [23]	✓	\times	0.3091	0.6558	9.313	2.695	0.383	0.571	0.680	0.882	3.736	0.020
MotionDiffuse [106]	✓	\times	0.2401	0.2703	7.710	0.138	0.426	0.616	0.723	0.563	3.392	0.320
MDM [86]	✓	\times	0.1011	1.7101	8.523	0.666	0.317	0.490	0.599	0.461	4.180	0.320
T2M-GPT [105]	✓	✓	0.1789	0.5241	6.162	1.176	0.394	0.576	0.683	0.269	3.710	0.190
MotionGPT [50]	✓	✓	0.6986	0.2245	7.889	2.271	0.128	0.208	0.271	1.020	7.055	0.389
ShapeMove (Ours)	✓	✓	0.0268	0.2658	6.143	0.625	0.413	0.601	0.705	0.198	3.533	0.117

4. Experiments

In this section, we begin by discussing the experimental setup in Section 4.1. We then introduce the baselines used for comparison and present the results in Section 4.2, which includes quantitative comparisons, qualitative evaluations, and human perceptual assessments.

4.1. Experimental Setup

Dataset. We use the current largest text-to-motion dataset, HumanML3D [43], which comprises 14,616 motion sequences and 44,970 motion descriptions. The motion sequences are sourced from 449 different subjects in AMASS [7, 19, 21, 31, 47, 49, 57, 59, 60, 64, 82, 89, 91, 92] and HumanAct12 [20]. We follow the same data preprocessing procedures outlined for HumanML3D, but we omit normalizing the motions to a canonical model to get shape-aware motions, as detailed in Section 3.1.

Implementation Details. To train the SA-VAE, we configure the level ℓ of the FSQ quantizer as $\ell = [8, 5, 5, 5]$, constructing a codebook that contains $k = 1000$ indices with each index dimension set to 512. During training, we crop motion sequences to a length $T = 64$ and set the down-sampled length $\tau = 16$. We employ the AdamW optimizer with $\beta_1 = 0.9$ and $\beta_2 = 0.99$ (following standard AdamW notation — no relation to the shape β), along with an exponential moving constant $\lambda = 0.99$. We train for 200K iterations at a learning rate of $2e^{-4}$, followed by 100K iterations at $1e^{-5}$. We set λ_f , λ_s , and λ_b to 10, and $q\%$ for data augmentation to 10%. With a batch size of 256, training takes approximately 12 hours on a single A100 GPU.

We use T5 [71] as our pretrained language model, which consists of 12 layers in both the transformer encoder and

Table 2. **Quantizer Reconstruction Comparison.** We report the reconstruction results, comparing our SA-VAE against baseline methods that utilize a VAE to quantize motion into discrete tokens. We assess the bone length difference, jitter score difference, and FID score relative to the shape-aware ground truth motions. Our VAE outperforms the baseline across all three metrics, particularly in reducing the bone length error by nearly half. These results demonstrate our model’s effectiveness in aligning with the physical form of different body shapes. █ and █ highlight the best and second-best results.

Methods	FID \downarrow	Bone Length Diff. (mm) \downarrow	Jitter Diff. (m/s^2) \downarrow
TM2T [44]	0.528	131.06	79.87
MotionGPT [50]	0.173	94.27	40.44
T2M-GPT [105]	0.151	83.42	34.75
SA-VAE (Ours)	0.125	45.88	31.49

decoder. We employ AdamW optimizer with $\beta_1 = 0.9$ and $\beta_2 = 0.99$ at a learning rate of $8e^{-4}$. We set λ_β to 0.5 and train the model for 120K iterations on two distinct tasks: text-to-motion and motion-to-text. With a batch size of 64, this training phase requires one day on 8 A100 GPUs. Subsequently, we train the model solely on the text-to-motion task using the same batch size and learning rate for an additional 30K steps, which takes 10 hours on 8 A100 GPUs.

Evaluation Metrics. To evaluate the physical plausibility of motions, we adopt the physics-based metrics of [88, 102]. The *Penetrate* metric measures ground penetration by computing the distance between the ground and the lowest body joints below the ground. *Float* measures the distance between the ground and the lowest body joints above the ground. *Skate* measures foot skating by computing the per-

Table 3. **Ablation Study.** *sc* stands for shape-conditioning.  and  highlight the best, second-best and third-best results.

Methods	FID ↓	Bone Length Diff. (mm) ↓	Float (cm) ↓	Skate (%) ↓
No sc	0.148	99.18	0.575	6.76
sc	 0.105	66.41	0.567	 6.60
sc+ L_{bone}	 0.107	 45.11	0.480	7.07
sc+ L_{bone} + L_{float}	0.137	 45.97	 0.255	7.90
sc+ L_{bone} + L_{float} + L_{skate} (Full)	 0.125	45.88	0.266	 6.14

Table 4. **Attributes Prediction.** We present the differences (cm) across six attributes between our beta predictions and the ground truth, focusing solely on our method as no comparable works predict beta concurrently. Our model demonstrates a robust ability to predict the correct beta values, with discrepancies from the ground truth around one cm. *C.* stands for circumference.

Attributes	Difference	Attributes	Difference	Attributes	Difference
Height	0.5767	Arm Length	0.0433	Leg Length	0.0505
Chest C.	0.6921	Waist C.	1.0558	Hip C.	0.6044

centage of frames where the foot joints in contact with the ground have a velocity over a threshold. We also propose a new metric, *Bone Length Variances*, which measures the variance of arm and leg lengths across the entire sequence to evaluate the stability of the generated motion. Following HUMOS [88], we exclude motions involving climbing and compute the *Penetrate*, *Float*, and *Skate* on the remaining dataset. This selection ensures the accuracy and relevance of the metrics for motions primarily characterized by ground-based dynamics.

We follow the evaluation protocol proposed by Guo *et al.* [43] to evaluate text-motion alignment and motion quality. *Fréchet Inception Distance (FID)* evaluates the distance of feature distributions between the generated and real motions. *R-Precision* evaluates the accuracy of matching between texts and motions using the top 1/2/3 retrieval accuracy. *Multimodal Distance (MM-Dist)* measures the feature distance between motions and texts. *Diversity* calculates the variance through features extracted from the motions. We compute all results with a 95% confidence interval obtained from 20 repeated runs.

4.2. Comparison with Baselines

We compare our results with the existing state-of-the-art approaches, including T2M [43], TM2T [44], MLD [23], MotionDiffuse [106], MDM [86], T2M-GPT [105], and MotionGPT [50]. We train these baseline methods using our training data, including shape and motion descriptions, and task the models to predict shape-aware motions. We note that T2M [43] and TM2T [44] employ a specific vocabulary for text encoder training and thus cannot incorporate shape descriptions as input. Therefore, we only input motion descriptions for these models and report the results

as a reference. In the following subsections, we present quantitative, qualitative, and perceptual evaluation results, demonstrating that our model achieves state-of-the-art performance across these metrics.

Quantitative Results. We present the physical plausibility comparison in Table 1. Our method outperforms baseline models that share the same settings, achieving the best performance in the *Penetrate*, *Skating*, and *Bone Length* metrics and ranking second best in the *Float* metric. This demonstrates our method’s effectiveness in learning physical rules. The metrics might not fully reflect the true realism of the generated motion for all motion scenarios. Hence, we also conduct a perception evaluation with human participants for a comprehensive assessment.

We also report results on text-motion alignment metrics in Table 1, where our model outperforms the same set of baselines across all metrics. Our model also achieves the best FID score over baselines, even outperforming baselines that require ground truth motion length during generation (which has limited practicality in real-world applications).

We report the quantizer performance in Table 2. TM2T [44], T2M-GPT [105], and MotionGPT [50], all quantize motions into discrete tokens. We present the performance of our SA-VAE in comparison with these models. From Table 2, we focus on the reconstruction quality of the model, emphasizing three metrics: the FID score to assess the motion quality, the bone length difference to measure the skeletal discrepancies between the reconstructed and ground truth motions, and the jitter difference to evaluate the disparity in the mean acceleration between reconstructed and ground truth motions. Our model demonstrates superior performance on all three metrics, achieving the lowest FID score and approximately half the bone length difference, which underscores the effectiveness of our SA-VAE in reconstructing shape-aware motions.

As we are the first, to the best of our knowledge, to predict shape parameters concurrently, we exclusively report the differences in body attributes. Table 4 presents these results, showing that our model can predict shape parameters differing by around 1 cm from the ground truth.

We also conduct an ablation study to evaluate the impact of the various components used in our model, including *shape-conditioning*, bone length loss L_{bone} , float loss L_{float} , and foot skate loss L_{skate} . We assess these variants on FID, bone length difference, floating, and foot skate ratio. Table 3 shows how each component improves performance across the metrics. We select our final model configurations as the one achieving the best overall results.

Qualitative Results. Figure 4 illustrates a qualitative comparison on two samples from the HumanML3D test set.

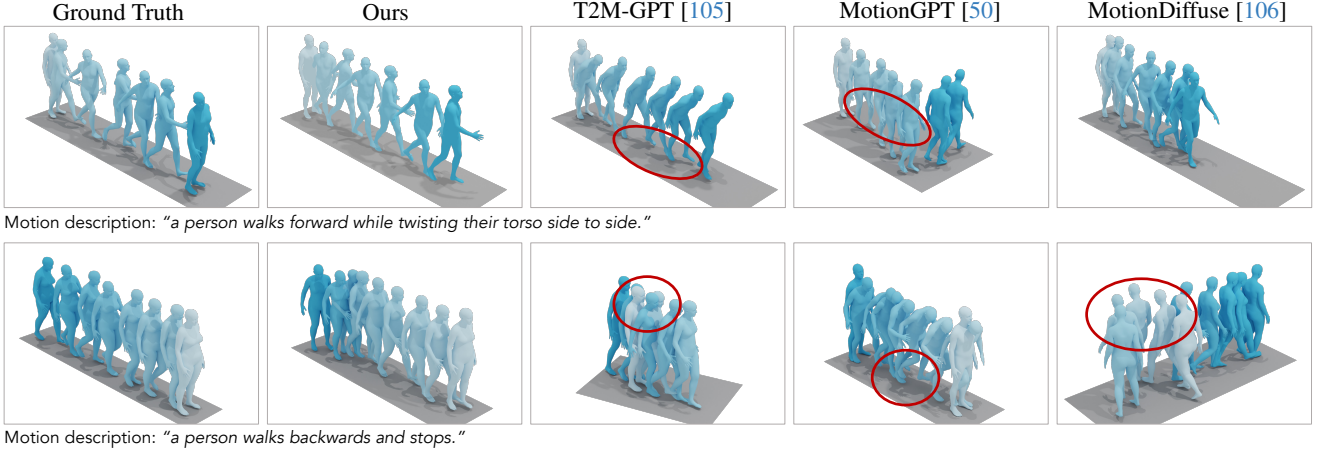


Figure 4. **Qualitative Comparisons.** We compare our method with three baseline methods, T2M-GPT [105], MotionGPT [50], and MotionDiffuse [106], illustrating two samples from the HumanML3D test set. The motions are colored from light to dark blue to represent progression over time. We highlight issues such as incorrect foot motion and other inaccuracies that do not align with expected motion patterns. Our method not only generates motions that align with the textual descriptions, but also accurately follows the body attributes and physical dynamics of the ground truth. Additional visual results and detailed comparisons are available in the project website.

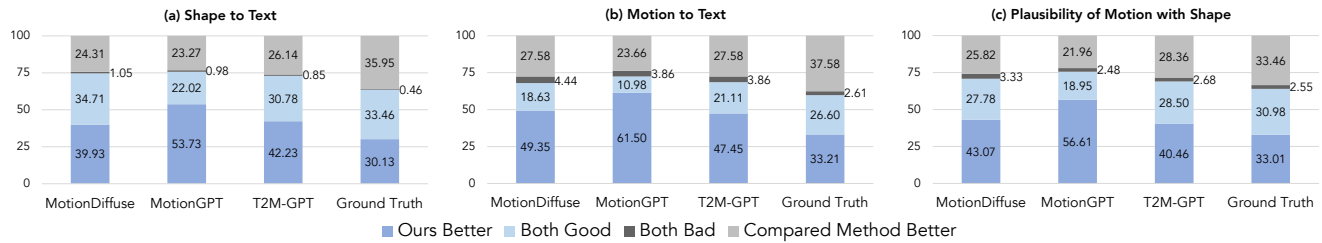


Figure 5. **Perceptual Evaluation.** We show the distributions of aggregate responses from annotators on their preferences for samples generated by our method and baseline methods, including MotionDiffuse [106], MotionGPT [50], and T2M-GPT [105], as well as the corresponding ground truth samples. We assess the distributions on three metrics: (a) *Shape to Text*, how well the body shape matches the text input; (b) *Motion to Text*, how well the motion matches the text input; and (c) *Plausibility of Motion with Shape*, how realistic the motions appear for the corresponding body shapes. Across all three metrics, we observe that our method is preferred nearly as much as the ground truth and is favored by approximately 12% to 38% over the baselines.

Our method can generate realistic motions that are well-aligned with both shape and motion descriptions. In contrast, body shapes in other methods are obtained indirectly via fitting the SMPL model to the generated joints. The red circles highlight unrealistic motions, such as floating feet, misaligned postures, incomplete actions, self-intersections, and deviating from the prompt. More visual results are available on the website.

Perceptual Evaluation. We conducted a human perceptual evaluation with pairwise comparisons between motion samples generated by our method and other baselines, as well as the corresponding ground truth samples. We selected the three best baselines from our quantitative evaluations, which also follow the same generation paradigm as ours, for comparison: MotionDiffuse [106],

MotionGPT [50], and T2M-GPT [105]. For each pairwise comparison, we show our sample and the other sample (one of the baselines or ground truth), for the same text description, in a random order to the participants. We ask them to rank the two samples as one of *sample 1 better, sample 2 better, both similarly good* or *both similarly bad* on three metrics: shape-to-text accuracy, motion-to-text accuracy, and plausibility of motion with shape. We randomly selected 34 text descriptions from the HumanML3D test set to generate the sample sets for the perceptual study, and recruited participants through Amazon Mechanical Turk. After filtering out inadmissible study responses (e.g., responses that were too quick and self-inconsistent), we report our perceptual evaluation results with 45 respondents in Figure 5. We note that our method was consistently preferred over the baselines and even matched the preference

rate of the ground truth.

5. Limitations

One limitation of our approach is the constrained nature of the shape descriptions used for motion generation. The pre-processing step requires descriptions to adhere to a specific template, which may restrict the model’s ability to handle various natural language inputs and diverse body shapes. This limitation could be mitigated by incorporating a more diverse dataset with a broader range of descriptive styles. Additionally, employing an advanced language model to preprocess and standardize descriptions to fit the required template can enhance the model’s versatility and real-world applicability.

6. Conclusions

We have presented a novel framework for shape-aware motion synthesis from textual descriptions, with the ability to generate both shape parameters and shape-aware motions from input text descriptions. Our method effectively captures the diverse correlations between human body shapes and motion dynamics, as evidenced by comprehensive evaluations that include quantitative results, qualitative comparisons, and perceptual studies with humans.

References

- [1] M. Abdul-Massih, I. Yoo, and B. Benes. Motion style retargeting to characters with different morphologies. *Computer Graphics Forum*, 36(6):86–99, 2017. [2](#)
- [2] Kfir Aberman, Rundi Wu, Dani Lischinski, Baoquan Chen, and Daniel Cohen-Or. Learning character-agnostic motion for motion retargeting in 2d. *ACM Trans. Graph.*, 38(4), 2019. [2](#)
- [3] Kfir Aberman, Peizhuo Li, Dani Lischinski, Olga Sorkine-Hornung, Daniel Cohen-Or, and Baoquan Chen. Skeleton-aware networks for deep motion retargeting. *ACM Trans. Graph.*, 39(4), 2020. [2](#)
- [4] Hyemin Ahn, Timothy Ha, Yunho Choi, Hwiyeon Yoo, and Songhwai Oh. Text2action: Generative adversarial synthesis from language to action. In *ICRA*, 2018. [3](#)
- [5] Chaitanya Ahuja and Louis-Philippe Morency. Language2pose: Natural language grounded pose forecasting. In *2019 International Conference on 3D Vision (3DV)*, pages 719–728, 2019. [2, 3](#)
- [6] Syed Muhammad Abrar Akber, Sadia Nishat Kazmi, Syed Muhammad Mohsin, and Agnieszka Szczęsna. Deep learning-based motion style transfer tools, techniques and future challenges. *Sensors*, 23(5), 2023. [2](#)
- [7] Ijaz Akhter and Michael J. Black. Pose-conditioned joint angle limits for 3D human pose reconstruction. In *CVPR*, 2015. [6](#)
- [8] Emre Aksan, Manuel Kaufmann, and Otmar Hilliges. Structured prediction helps 3d human motion modelling. In *ICCV*, 2019. [2](#)
- [9] Sadegh Aliakbarian, Fatemeh Sadat Saleh, Mathieu Salzmann, Lars Petersson, and Stephen Gould. A stochastic conditioning scheme for diverse human motion prediction. In *CVPR*, 2020. [3](#)
- [10] Nikos Athanasiou, Mathis Petrovich, Michael J. Black, and GÜl Varol. TEACH: Temporal Action Compositions for 3D Humans. In *3DV*, 2022. [3](#)
- [11] Nikos Athanasiou, Mathis Petrovich, Michael J. Black, and GÜl Varol. Sinc: Spatial composition of 3d human motions for simultaneous action generation. In *ICCV*, 2023. [3](#)
- [12] Fan Bao, Chongxuan Li, Jun Zhu, and Bo Zhang. Analytic-DPM: an analytic estimate of the optimal reverse variance in diffusion probabilistic models. In *ICLR*, 2022. [2](#)
- [13] Emad Barsoum, John Kender, and Zicheng Liu. Hp-gan: Probabilistic 3d human motion prediction via gan. In *CVPR Workshops*, 2018. [3](#)
- [14] Jean Basset, Stefanie Wuhrer, Edmond Boyer, and Franck Multon. Contact preserving shape transfer for rigging-free motion retargeting. In *ACM SIGGRAPH Conference on Motion, Interaction and Games*, 2019. [2](#)
- [15] Kevin Bergamin, Simon Clavet, Daniel Holden, and James Richard Forbes. Drecon: data-driven responsive control of physics-based characters. *ACM Trans. Graph.*, 38(6), 2019. [2](#)
- [16] Aneesh Bhattacharya, Manas Paranjape, Uttaran Bhattacharya, and Aniket Bera. Danceanyway: synthesizing beat-guided 3d dances with randomized temporal contrastive learning. In *Proceedings of the Thirty-Eighth AAAI Conference on Artificial Intelligence*. AAAI Press, 2024. [2](#)
- [17] Uttaran Bhattacharya, Elizabeth Childs, Nicholas Rewkowski, and Dinesh Manocha. Speech2affectivegestures: Synthesizing co-speech gestures with generative adversarial affective expression learning. In *ACM MM*, 2021. [2](#)
- [18] Uttaran Bhattacharya, Nicholas Rewkowski, Abhishek Banerjee, Pooja Guhan, Aniket Bera, and Dinesh Manocha. Text2gestures: A transformer-based network for generating emotive body gestures for virtual agents. In *Virtual Reality and 3D User Interfaces (VR)*, 2021. [2](#)
- [19] Federica Bogo, Javier Romero, Gerard Pons-Moll, and Michael J. Black. Dynamic FAUST: Registering human bodies in motion. In *CVPR*, 2017. [6](#)
- [20] Judith Butepage, Michael J Black, Danica Kragic, and Hedvig Kjellstrom. Deep representation learning for human motion prediction and classification. In *CVPR*, 2017. [6](#)
- [21] Carnegie Mellon University. CMU MoCap Dataset, 2003. [6](#)
- [22] Ufuk Celikcan, Ilker O. Yaz, and Tolga Capin. Example-Based Retargeting of Human Motion to Arbitrary Mesh Models. *Computer Graphics Forum*, 2015. [2](#)
- [23] Xin Chen, Biao Jiang, Wen Liu, Zilong Huang, Bin Fu, Tao Chen, and Gang Yu. Executing your commands via motion diffusion in latent space. In *CVPR*, 2023. [3, 6, 7](#)
- [24] Kwang-Jin Choi and Hyeong-Seok Ko. Online motion retargetting. *The Journal of Visualization and Computer Animation*, 11(5):223–235, 2000. [2](#)

[25] Vasileios Choutas, Lea Müller, Chun-Hao P Huang, Siyu Tang, Dimitrios Tzionas, and Michael J Black. Accurate 3d body shape regression using metric and semantic attributes. In *CVPR*, 2022. 3, 4

[26] Rishabh Dabral, Muhammad Hamza Mughal, Vladislav Golyanik, and Christian Theobalt. Mofusion: A framework for denoising-diffusion-based motion synthesis. In *CVPR*, 2023. 3

[27] Unreal Engine. dev.epicgames.com/documentation/en-us/unreal-engine/animation-retargeting-in-unreal-engine, 2015. 1, 2

[28] Yao Feng, Jing Lin, Sai Kumar Dwivedi, Yu Sun, Priyanka Patel, and Michael J. Black. ChatPose: Chatting about 3d human pose. In *CVPR*, 2024. 5

[29] Katerina Fragkiadaki, Sergey Levine, Panna Felsen, and Jitendra Malik. Recurrent network models for human dynamics. In *ICCV*, 2015. 2

[30] Levi Fussell, Kevin Bergamin, and Daniel Holden. Supertrack: motion tracking for physically simulated characters using supervised learning. *ACM Trans. Graph.*, 40(6), 2021. 2

[31] Saeed Ghorbani, Kimia Mahdaviani, Anne Thaler, Konrad Kording, Douglas James Cook, Gunnar Blohm, and Nikolaus F. Troje. MoVi: A large multipurpose motion and video dataset. *arXiv preprint arXiv: 2003.01888*, 2020. 6

[32] Anindita Ghosh, Noshaba Cheema, Cennet Oguz, Christian Theobalt, and Philipp Slusallek. Synthesis of compositional animations from textual descriptions. In *ICCV*, 2021. 2

[33] Anindita Ghosh, Noshaba Cheema, Cennet Oguz, Christian Theobalt, and Philipp Slusallek. Text-based motion synthesis with a hierarchical two-stream rnn. In *ACM SIGGRAPH 2021 Posters*, New York, NY, USA, 2021. Association for Computing Machinery. 2

[34] Anindita Ghosh, Rishabh Dabral, Vladislav Golyanik, Christian Theobalt, and Philipp Slusallek. Imos: Intent-driven full-body motion synthesis for human-object interactions. *Computer Graphics Forum*, 42(2):1–12, 2023. 3

[35] Anindita Ghosh, Rishabh Dabral, Vladislav Golyanik, Christian Theobalt, and Philipp Slusallek. Remos: 3d motion-conditioned reaction synthesis for two-person interactions. In *ECCV*, 2024. 2

[36] Partha Ghosh, Jie Song, Emre Aksan, and Otmar Hilliges. Learning human motion models for long-term predictions. In *3DV*, 2017. 2

[37] Shiry Ginosar, Amir Bar, Gefen Kohavi, Caroline Chan, Andrew Owens, and Jitendra Malik. Learning individual styles of conversational gesture. In *CVPR*, 2019. 2

[38] Thiago L. Gomes, Renato Martins, João Ferreira, Rafael Azevedo, Guilherme Torres, and Erickson R. Nascimento. A shape-aware retargeting approach to transfer human motion and appearance in monocular videos. *Int. J. Comput. Vision*, 129(7):2057–2075, 2021. 2

[39] Anand Gopalakrishnan, Ankur Mali, Dan Kifer, Lee Giles, and Alexander G. Ororbia. A neural temporal model for human motion prediction. In *CVPR*, 2019. 2

[40] Omer Gralnik, Guy Gafni, and Ariel Shamir. Semantify: Simplifying the control of 3d morphable models using clip. In *ICCV*, 2023. 3

[41] Ulf Grenander and Michael I. Miller. Representations of knowledge in complex systems. *Journal of the Royal Statistical Society: Series B (Methodological)*, 56(4):549–581, 1994. 2

[42] Chuan Guo, Xinxin Zuo, Sen Wang, Shihao Zou, Qingyao Sun, Annan Deng, Minglun Gong, and Li Cheng. Action2motion: Conditioned generation of 3d human motions. In *ACM MM*, 2020. 2

[43] Chuan Guo, Shihao Zou, Xinxin Zuo, Sen Wang, Wei Ji, Xingyu Li, and Li Cheng. Generating diverse and natural 3d human motions from text. In *CVPR*, 2022. 3, 4, 6, 7

[44] Chuan Guo, Xinxin Zuo, Sen Wang, and Li Cheng. Tm2t: Stochastic and tokenized modeling for the reciprocal generation of 3d human motions and texts. In *ECCV*, 2022. 3, 4, 6, 7

[45] Chuan Guo, Yuxuan Mu, Muhammad Gohar Javed, Sen Wang, and Li Cheng. Momask: Generative masked modeling of 3d human motions. In *CVPR*, 2023. 3

[46] Chengan He, Jun Saito, James Zachary, Holly Rushmeier, and Yi Zhou. Nemf: Neural motion fields for kinematic animation. In *NIPS*, 2022. 3

[47] Fabian Helm, Nikolaus Troje, Mathias Reiser, and Jörn Munzert. Bewegungsanalyse getäuschter und nicht-getäuschter 7m-würfe im handball. *47. Jahrestagung der Arbeitsgemeinschaft für Sportpsychologie, Freiburg.*, 2015. 6

[48] Daniel Holden, Jun Saito, and Taku Komura. A deep learning framework for character motion synthesis and editing. *ACM Trans. Graph.*, 35(4), 2016. 2

[49] Ludovic Hoyet, Kenneth Ryall, Rachel McDonnell, and Carol O’Sullivan. Sleight of hand: Perception of finger motion from reduced marker sets. In *ACM SIGGRAPH Symposium on Interactive 3D Graphics and Games*, 2012. 6

[50] Biao Jiang, Xin Chen, Wen Liu, Jingyi Yu, Gang Yu, and Tao Chen. Motiogpt: Human motion as a foreign language. *NIPS*, 2024. 2, 3, 4, 6, 7, 8

[51] Nan Jiang, Zhiyuan Zhang, Hongjie Li, Xiaoxuan Ma, Zan Wang, Yixin Chen, Tengyu Liu, Yixin Zhu, and Siyuan Huang. Scaling up dynamic human-scene interaction modeling. In *CVPR*, 2024. 3

[52] Taku Komura, Ikhсанul Habibie, Daniel Holden, Jonathan Schwarz, and Joe Yearsley. A recurrent variational autoencoder for human motion synthesis. In *BMVC*, 2017. 2

[53] Xin Lai, Zhuotao Tian, Yukang Chen, Yanwei Li, Yuhui Yuan, Shu Liu, and Jiaya Jia. Lisa: Reasoning segmentation via large language model. In *CVPR*, 2024. 5

[54] Sunmin Lee, Taeho Kang, Jungnam Park, Jehee Lee, and Jungdam Won. Same: Skeleton-agnostic motion embedding for character animation. In *SIGGRAPH Asia Conference Papers*, 2023. 2

[55] Rui long Li, Shan Yang, David A. Ross, and Angjoo Kanazawa. Ai choreographer: Music conditioned 3d dance generation with aist++. In *ICCV*, 2021. 2

[56] Matthew Loper, Naureen Mahmood, Javier Romero, Gerard Pons-Moll, and Michael J. Black. Smpl: a skinned multi-person linear model. *ACM Trans. Graph.*, 34(6), 2015. 3

[57] Matthew M. Loper, Naureen Mahmood, and Michael J. Black. MoSh: Motion and shape capture from sparse markers. *ACM Transactions on Graphics, (Proc. SIGGRAPH Asia)*, 33(6):220:1–220:13, 2014. 6

[58] Zhenyu Lou, Qiongjie Cui, Haofan Wang, Xu Tang, and Hong Zhou. Multimodal sense-informed forecasting of 3d human motions. In *CVPR*, 2024. 3

[59] Eyes JAPAN Co. Ltd. Eyes Japan MoCap Dataset, 2008. 6

[60] Naureen Mahmood, Nima Ghorbani, Nikolaus F. Troje, Gerard Pons-Moll, and Michael J. Black. AMASS: Archive of motion capture as surface shapes. In *ICCV*, 2019. 3, 6

[61] Viktor Makoviychuk, Lukasz Wawrzyniak, Yunrong Guo, Michelle Lu, Kier Storey, Miles Macklin, David Hoeller, Nikita Rudin, Arthur Allshire, Ankur Handa, and Gavriel State. Isaac gym: High performance GPU based physics simulation for robot learning. In *NIPS Datasets and Benchmarks Track*, 2021. 2

[62] Fabian Mentzer, David Minnen, Eirikur Agustsson, and Michael Tschannen. Finite scalar quantization: Vq-vae made simple, 2023. 3, 4

[63] MotionBuilder. autodesk.com/products/motionbuilder/overview, 2023. 1, 2

[64] M. Müller, T. Röder, M. Clausen, B. Eberhardt, B. Krüger, and A. Weber. Documentation mocap database hdm05. Technical Report CG-2007-2, Universität Bonn, 2007. 6

[65] Xue Bin Peng and Michiel van de Panne. Learning locomotion skills using deeprl: does the choice of action space matter? In *ACM SIGGRAPH SCA*, 2017. 2

[66] Xue Bin Peng, Pieter Abbeel, Sergey Levine, and Michiel van de Panne. Deepmimic: example-guided deep reinforcement learning of physics-based character skills. *ACM Trans. Graph.*, 37(4), 2018.

[67] Xue Bin Peng, Angjoo Kanazawa, Jitendra Malik, Pieter Abbeel, and Sergey Levine. Sfv: reinforcement learning of physical skills from videos. *ACM Trans. Graph.*, 37(6), 2018. 2

[68] Mathis Petrovich, Michael J. Black, and Gül Varol. Action-conditioned 3D human motion synthesis with transformer VAE. In *ICCV*, 2021. 3

[69] Mathis Petrovich, Michael J. Black, and Gül Varol. TEMOS: Generating diverse human motions from textual descriptions. In *ECCV*, 2022. 3

[70] Matthias Plappert, Christian Mandery, and Tamim Asfour. The KIT motion-language dataset. *Big Data*, 4(4):236–252, 2016. 3

[71] Colin Raffel, Noam Shazeer, Adam Roberts, Katherine Lee, Sharan Narang, Michael Matena, Yanqi Zhou, Wei Li, and Peter J. Liu. Exploring the limits of transfer learning with a unified text-to-text transformer. *Journal of Machine Learning Research*, 21(140):1–67, 2020. 6

[72] João Regateiro and Edmond Boyer. Temporal shape transfer network for 3d human motion. In *3DV*, 2022. 2

[73] Davis Rempe, Tolga Birdal, Aaron Hertzmann, Jimei Yang, Srinath Sridhar, and Leonidas J. Guibas. Humor: 3d human motion model for robust pose estimation. In *ICCV*, 2021. 3

[74] Zhiyuan Ren, Zhihong Pan, Xin Zhou, and Le Kang. Diffusion motion: Generate text-guided 3d human motion by diffusion model. In *ICASSP*, 2023. 3

[75] Rokoko. rokoko.com, 2023. 1, 2

[76] Alessio Sampieri, Alessio Palma, Indro Spinelli, and Fabio Galasso. Length-aware motion synthesis via latent diffusion. In *ECCV*, 2024. 3

[77] John Schulman, Philipp Moritz, Sergey Levine, Michael I. Jordan, and P. Abbeel. High-dimensional continuous control using generalized advantage estimation. In *ICLR*, 2016. 2

[78] John Schulman, Filip Wolski, Prafulla Dhariwal, Alec Radford, and Oleg Klimov. Proximal policy optimization algorithms. *arXiv preprint arXiv:1707.06347*, 2017. 2

[79] Yoni Shafir, Guy Tevet, Roy Kapon, and Amit Haim Bermano. Human motion diffusion as a generative prior. In *ICLR*, 2024. 3

[80] Soshi Shimada, Vladislav Golyanik, Weipeng Xu, and Christian Theobalt. Physcap: physically plausible monocular 3d motion capture in real time. *ACM Trans. Graph.*, 39(6), 2020. 2

[81] Soshi Shimada, Vladislav Golyanik, Weipeng Xu, Patrick Pérez, and Christian Theobalt. Neural monocular 3d human motion capture with physical awareness. *ACM Trans. Graph.*, 40(4), 2021. 2

[82] L. Sigal, A. Balan, and M. J. Black. HumanEva: Synchronized video and motion capture dataset and baseline algorithm for evaluation of articulated human motion. *International Journal of Computer Vision*, 87(1):4–27, 2010. 6

[83] Sebastian Starke, Yiwei Zhao, Taku Komura, and Kazi Zaman. Local motion phases for learning multi-contact character movements. *ACM Trans. Graph.*, 39(4), 2020. 1

[84] Kewei Sui, Anindita Ghosh, Inwoo Hwang, Jian Wang, and Chuan Guo. A survey on human interaction motion generation. *arXiv preprint arXiv:2503.12763*, 2025. 2

[85] Guy Tevet, Brian Gordon, Amir Hertz, Amit H Bermano, and Daniel Cohen-Or. Motionclip: Exposing human motion generation to clip space. In *ECCV*, 2022. 2, 3

[86] Guy Tevet, Sigal Raab, Brian Gordon, Yoni Shafir, Daniel Cohen-or, and Amit Haim Bermano. Human motion diffusion model. In *ICLR*, 2023. 3, 6, 7

[87] Shashank Tripathi, Lea Müller, Chun-Hao P. Huang, Omid Taheri, Michael J. Black, and Dimitrios Tzionas. 3d human pose estimation via intuitive physics. In *CVPR*, 2023. 2

[88] Shashank Tripathi, Omid Taheri, Christoph Lassner, Michael Black, Daniel Holden, and Carsten Stoll. Humos: Human motion model conditioned on body shape. In *ECCV*, 2024. 3, 5, 6, 7

[89] Matt Trumble, Andrew Gilbert, Charles Malleson, Adrian Hilton, and John Collomosse. Total Capture: 3d human pose estimation fusing video and inertial sensors. In *BMVC*, 2017. 6

[90] Jonathan Tseng, Rodrigo Castellon, and Karen Liu. Edge: Editable dance generation from music. In *CVPR*, 2023. 5

[91] ACCAD/Ohio State University. Advanced Computing Center for the Arts and Design, 2024. 6

[92] Simon Fraser University and National University of Singapore. SFU Motion Capture Database, 2011. 6

[93] Aaron Van Den Oord, Oriol Vinyals, et al. Neural discrete representation learning. In *NIPS*, 2017. 3

[94] Ruben Villegas, Duygu Ceylan, Aaron Hertzmann, Jimei Yang, and Jun Saito. Contact-aware retargeting of skinned motion. In *ICCV*, 2021. [2](#)

[95] Jiashun Wang, Chao Wen, Yanwei Fu, Haitao Lin, Tianyun Zou, Xiangyang Xue, and Yinda Zhang. Neural pose transfer by spatially adaptive instance normalization. In *CVPR*, 2020. [2](#)

[96] Jungdam Won, Deepak Gopinath, and Jessica Hodgins. A scalable approach to control diverse behaviors for physically simulated characters. *ACM Trans. Graph.*, 39(4), 2020. [2](#)

[97] Katsu Yamane, Yuka Ariki, and Jessica Hodgins. Animating Non-Humanoid Characters with Human Motion Data. In *ACM SIGGRAPH SCA*, 2010. [2](#)

[98] Xinyu Yi, Yuxiao Zhou, Marc Habermann, Soshi Shimada, Vladislav Golyanik, Christian Theobalt, and Feng Xu. Physical inertial poser (pip): Physics-aware real-time human motion tracking from sparse inertial sensors. In *CVPR*, 2022. [2](#)

[99] Ye Yuan and Kris Kitani. Dlow: Diversifying latent flows for diverse human motion prediction. In *ECCV*, 2020.

[100] Ye Yuan and Kris Kitani. Residual force control for agile human behavior imitation and extended motion synthesis. In *NIPS*, 2020.

[101] Ye Yuan, Shih-En Wei, Tomas Simon, Kris Kitani, and Jason Saragih. Simpoe: Simulated character control for 3d human pose estimation. In *CVPR*, 2021. [2](#)

[102] Ye Yuan, Jiaming Song, Umar Iqbal, Arash Vahdat, and Jan Kautz. Physdiff: Physics-guided human motion diffusion model. In *ICCV*, 2023. [5](#), [6](#)

[103] Petrissa Zell, Bastian Wandt, and Bodo Rosenhahn. Joint 3d human motion capture and physical analysis from monocular videos. In *CVPR Workshops*, 2017. [2](#)

[104] Jiaxu Zhang, Junwu Weng, Di Kang, Fang Zhao, Shaoli Huang, Xuefei Zhe, Linchao Bao, Ying Shan, Jue Wang, and Zhigang Tu. Skinned motion retargeting with residual perception of motion semantics & geometry. In *CVPR*, 2023. [2](#)

[105] Jianrong Zhang, Yangsong Zhang, Xiaodong Cun, Shaoli Huang, Yong Zhang, Hongwei Zhao, Hongtao Lu, and Xi Shen. T2m-gpt: Generating human motion from textual descriptions with discrete representations. In *CVPR*, 2023. [2](#), [3](#), [4](#), [5](#), [6](#), [7](#), [8](#)

[106] Mingyuan Zhang, Zhongang Cai, Liang Pan, Fangzhou Hong, Xinying Guo, Lei Yang, and Ziwei Liu. Motiondifuse: Text-driven human motion generation with diffusion model. *arXiv preprint arXiv:2208.15001*, 2022. [3](#), [6](#), [7](#), [8](#)

[107] Zeyu Zhang, Akide Liu, Ian Reid, Richard Hartley, Bohan Zhuang, and Hao Tang. Motion mamba: Efficient and long sequence motion generation. In *ECCV*, 2024. [3](#)

[108] Keyang Zhou, Bharat Lal Bhatnagar, and Gerard Pons-Moll. Unsupervised shape and pose disentanglement for 3d meshes. In *ECCV*, 2020. [2](#)

[109] Baldomero R. Árbol and Dan Casas. Bodyshapegpt: Smpl body shape manipulation with llms. In *ECCV Workshop on Foundation Models for 3D Humans*, 2024. [3](#)